Available online at www.sciencedirect.com
SCIENCE DIRECT®
Journal of Computational and Applied Mathematics 175 (2005) 429–446
JOURNAL OF COMPUTATIONAL AND APPLIED MATHEMATICS
www.elsevier.com/locate/cam

Numerical simulation of stochastic PDEs for excitable media

Tony Shardlow*

Department of Mathematics, University of Manchester, Oxford Road, Manchester M13 9PL, UK

Received 1 December 2003; received in revised form 28 June 2004

Abstract

We discuss the numerical solution of a number of stochastic perturbations of the Barkley model of excitable media, widely used in the study of spiral waves. Two numerical methods are considered for solving this equation, one based on Barkley's original formulation and one based on spectral methods. It is found to be beneficial to modify the nonlinearity describing the reaction kinetics. An efficient method of approximating the Wiener process is presented. The effectiveness of the methods depends on the stochastic PDE under consideration.

MSC: 35K57; 60H15; 60H35; 65

Keywords: Reaction-diffusion equations; Stochastic PDEs; Excitable media; Computations; Numerical analysis

1. Introduction

In recent years, much work has been devoted to understanding waves in excitable media, motivated by a wealth of natural systems that exhibit spiral waves [25]. One example is the heart, where waves of electrical activity propagate in cardiac muscle to stimulate the heartbeat; irregularities in the cardiac rhythm, such as fibrillations, are related to the self-sustaining activity of spiral and scroll waves [16]. There are many other examples, such as the Belousov–Zhabotinsky chemical reaction [26] and the patterns of slime mould amoebae [23]. Two basic features are common to models of excitable media: spatially localised excitation which (i) diffuses in space and (ii) falls into a recovery state after a short time. Cellular automata and PDEs can be used to model excitable media.

* Tel.: +44-161-275-5821; fax: +44-161-275-5819.
E-mail address: shardlow@maths.man.ac.uk (T. Shardlow).

0377-0427/$ - see front matter © 2004 Elsevier B.V. All rights reserved.
doi:10.1016/j.cam.2004.06.020

Cellular automata models include the Wiener–Rosenbluth [24] and Greenberg–Hastings models [13]. The Greenberg–Hastings model is posed on a lattice with state X_{ij} at site $(i, j) \in \mathbf{Z}^2$ that takes discrete values corresponding to one quiescent, E excitable, and R refractory states. A quiescent state becomes excited when a nearest neighbours is excited. An excited state cycles through the E excited states, and then becomes refractory. A refractory site cycles through the R refractory states and then becomes quiescent. Cellular automata are simple to solve computationally, but most models fail to model curvature effects that are important in spiral wave motion.

PDE models overcome some of the drawbacks of cellular automata. Two well-known PDEs are the FitzHugh–Nagumo [9] and the Barkley [2] equations. We focus on the simpler Barkley PDE, which is for excitation field u and inhibitor field v:

$$\begin{aligned} \frac{\partial u}{\partial t} &= D\nabla^2 u + f(u, v)/\varepsilon, \\ \frac{\partial v}{\partial t} &= g(u, v), \end{aligned} \tag{1.1}$$

for diffusion coefficient D, where initial conditions are specified for u and v at $t = 0$ and boundary conditions are applied on the domain $[0, L]^2$ (usually, periodic or Neumann conditions). The parameter $\varepsilon > 0$ is small and controls the separation of the excitation and inhibitor time scales. The reaction terms

$$f(u, v) = u(1 - u)\left(u - \frac{v + b}{a}\right), \quad g(u, v) = u - v \tag{1.2}$$

for $a, b > 0$. Typical values are $a = 0.75$ and $b = 0.01$. The reaction kinetics are understood from the (u, v) phase plane of the corresponding ODE

$$\frac{\partial u}{\partial t} = f(u, v)/\varepsilon, \quad \frac{\partial v}{\partial t} = g(u, v). \tag{1.3}$$

See Fig. 1. The key feature is the heteroclinic orbit leading to $u = v = 0$. A small perturbation from the stable zero state causes a large excursion, which models the excited ($u \approx 1$) and refractory ($v \approx 1$) cycle. Adding in spatial diffusion to this reaction kinetics yields spiral wave dynamics.

A number of stochastic perturbations of these models have been introduced in the literature. The earliest is perhaps [20], where the recovery time is distributed randomly over space in a cellular automata. Another type of stochastic perturbation is [5], where spatial inhomogeneities in diffusion are added to FitzHugh–Nagumo and Greenberg–Hastings to model diseased heart tissue. In this paper, we are concerned with the effect of forcing the PDE (1.1) by a space-time Wiener process.

The simplest such perturbation is adding noise to the u field as

$$\begin{aligned} \mathrm{d}u &= [D\nabla^2 u + f(u, v)/\varepsilon]\,\mathrm{d}t + \sigma\,\mathrm{d}W(t, \mathbf{x}), \\ \mathrm{d}v &= g(u, v)\,\mathrm{d}t, \end{aligned} \tag{1.4}$$

where $\sigma \in \mathbf{R}$ is the noise intensity and $W(t, \mathbf{x})$ is a Wiener process to be specified (see (2.1) below). Discrete versions of this type of model, where additive noise stimulates the level of excitation is found in

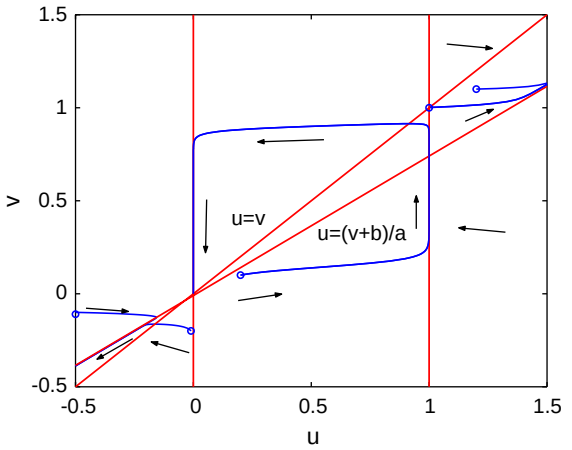

Fig. 1. Illustration of dynamics of $\frac{du}{dt} = f(u, v)/\varepsilon$, $\frac{dv}{dt} = g(u, v)$ for $a = 0.75$, $b = 0.01$, $\varepsilon = 0.02$. The arrows illustrate the vector field. The four nullclines are plotted. For initial condition $(0.2, 0.1)$, the system becomes excited and takes a large excursion before approaching the stable fixed point 0. For initial condition $(1.2, 1.1)$, the solution diverges to infinity along the line $u = (v + b)/a$.

[4,15]. Nucleation of waves results in this model from the background noise in the excitation level u, even from the homogeneous state $u = v = 0$. This is demonstrated in Figs. 2 and 3. Fig. 2 shows an example where a target wave is nucleated and Fig. 3 an example where a spiral is nucleated. This behaviour is related to the size of ε and is analysed further in [22].

A number of authors have suggested stochastic PDEs that exhibit stochastic resonance. For example, the following is considered by [1] for a function $h(u)$:

$$\begin{aligned} du &= [D\nabla^2 u + f(u, v)/\varepsilon]\,dt + h(u)\,dW(t, \mathbf{x}), \\ dv &= g(u, v)\,dt \end{aligned} \tag{1.5}$$

(where the equation is interpreted in the Itô sense) and the following by [6]:

$$\begin{aligned} du &= [D\nabla^2 u + f(u, v)/\varepsilon]\,dt, \\ dv &= g(u, v)\,dt + \sigma\,dW(t, \mathbf{x}). \end{aligned} \tag{1.6}$$

Space time stochastic resonance (STSR) has been observed in these systems. This means that waves are sustained even for parameters values that do not support such behaviour in the deterministic model. In particular, a sharp peak in the level of coherence (as measured by mutual information) of the spatial structures is observed as the parameters describing the noise is varied (typically, intensities and correlation lengths).

Another variation is the following Itô stochastic PDE [12]:

$$\begin{aligned} du &= [D\nabla^2 u + f(u, v)/\varepsilon]\,dt, \\ dv &= g(u, v)\,dt + u\sigma\,dW(t, \mathbf{x}). \end{aligned} \tag{1.7}$$

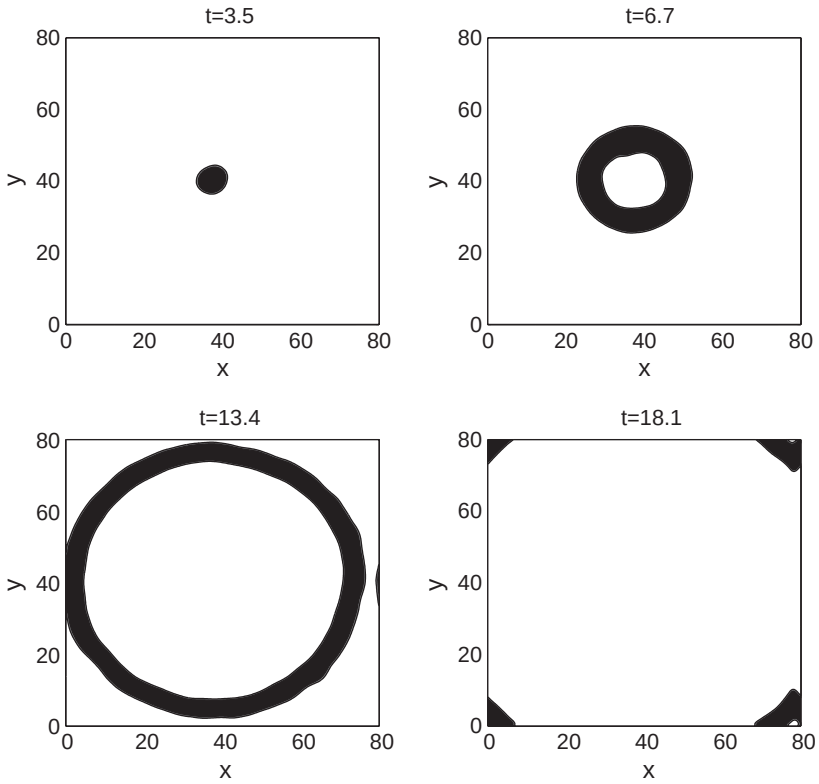

Fig. 2. Nucleation of a target pattern for (1.4) with $a = 0.75$, $b = 0.01$, $\varepsilon = 0.03$, $L = 80$ and noise has correlation length $\xi = 2$ and intensity $\sigma = 0.09$. The left hand plot shows a realisation of the u field (black indicates $u \approx 1$, white $u \approx 0$).

In this case, one of the rate parameters in the v equation is replaced by a random process. This model exhibits break down of spiral patterns, by "backfiring", spirals throw of new wave forms which interact and break up existing patterns. This process is shown in Fig. 4.

The numerical solution of models (1.4) and (1.7) are considered in this paper. The remainder of the paper is organised as follows. In Section 2, the stochastic PDEs are precisely formulated. The reaction terms are first considered. Due to an inherent instability in the reaction terms, easily stimulated in the presence of noise, we modify the reaction terms. The Wiener process is rigorously defined and motivated. We choose a noise white in time, but with exponentially decaying correlations in space. In Section 3, we formulate the numerical methods and discuss their performance. The two methods we consider are (i) Barkley's method [2], which is a finite difference method with a very efficient and effective approximation to the Laplacian, and (ii) a spectral approximation. In both cases, we provide an efficient method for simulating the noise, exploiting the rapid decay properties of the Fourier coefficients of the noise. In Section 4 and 5, we present some comments on the numerical solution of (1.7) and conclusions.

2. Formulation of a stochastic PDE

We formulate precisely the stochastic PDEs that we study. The first task is to consider the choice of reaction term. Solutions of ODE (1.3) diverge to infinity for certain initial data, for example in

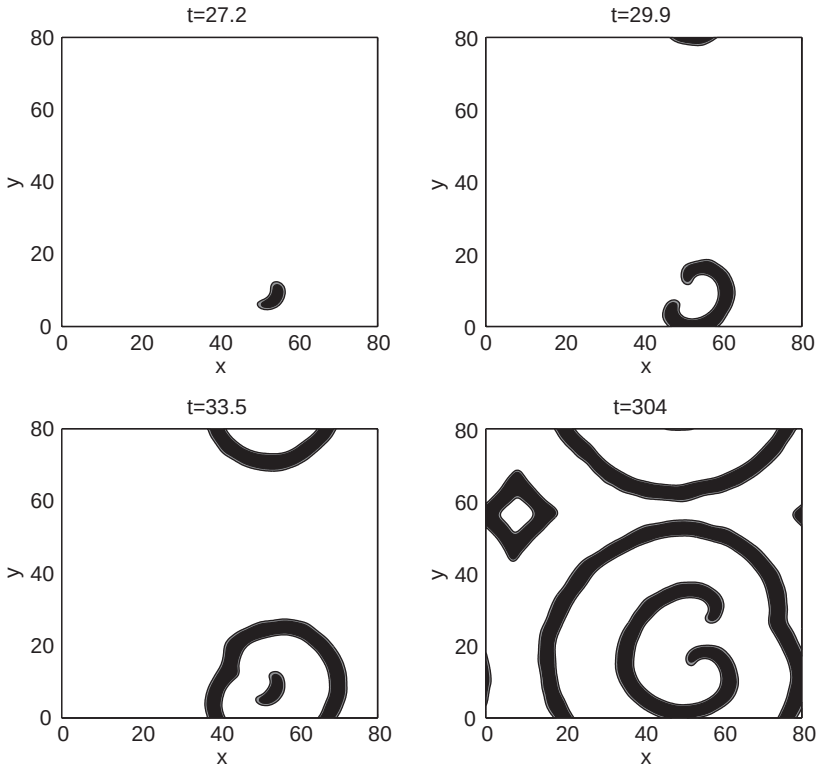

Fig. 3. Nucleation of a spiral pattern, with parameters as in Fig. 2 except for $\varepsilon = 0.05$ and $\sigma = 0.125$.

Fig. 1 the initial data $(u_0, v_0) = (1.2, 1.1)$ diverges along the line $u = (v + b)/a$. This behaviour is not apparent to those interested in deterministic models, as initial data is chosen within an invariant region: if $0 \leqslant u_0(\mathbf{x}), v_0(\mathbf{x}) \leqslant 1$, then $0 \leqslant u(t, \mathbf{x}), v(t, \mathbf{x}) \leqslant 1$ for $t \geqslant 0$. When forcing the model by an additive noise as in (1.4), the variable u can be kicked into any part of phase space, which may stimulate the divergent behaviour. This appears when simulating equation (1.4) numerically. This divergence can be seen in Fig. 5, where the $\| u \|_\infty$ is plotted against time. The numerically simulated divergence may be a numerical artifact, as the diffusion may control the growth in u when the model is more accurately discretised. However, numerical experiments with the method described in [8] indicate that the divergence is problematic even with an implicit update rule for (1.4).

The reaction terms can be modified such that the basic mechanisms of the excitable media are not changed, but the model remains well-behaved—the excitation level u remains close to the interval $[0, 1]$—when some noise is added. One way of doing this is

$$\tilde{f}(u, v) = \begin{cases} f(u, v), & u \leqslant 1, \\ -|f(u, v)|, & u \geqslant 1, \end{cases} \qquad \tilde{g}(u, v) = \begin{cases} g(u, v), & v \geqslant 0, \\ |g(u, v)|, & v < 0. \end{cases}$$

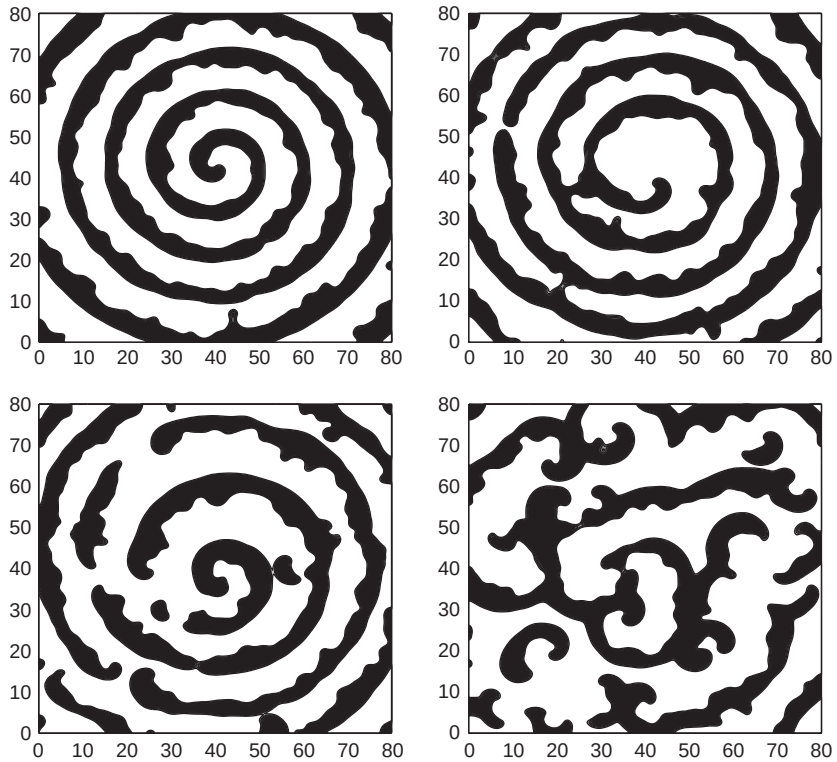

Fig. 4. Plots of the u field in a numerical simulation of (1.7) with parameter values $a=0.75$, $b=0.01$, $D=1$, $L=80$, $\varepsilon=0.03$, $\sigma=1$, and correlation length $\xi=2$. The resolution is 256^2 grid points with time step 0.02. Time runs from top left to bottom right and figures are separated by 8 time units.

The (u, v) phase plane for the corresponding ODE system is shown in Fig. 6. In this case, the trajectories are bounded for all initial data, while the heteroclinic orbit is unchanged. This modified nonlinearity is used in the numerical experiments presented in this paper.

We will now be precise about the choice of Wiener process $W(t, \mathbf{x})$. We wish the process to be convenient for numerical simulation and in particular it will be convenient to generate the process using Fast Fourier Transforms. To develop this, we work with homogeneous Neumann boundary conditions, though periodic conditions would suit equally well. Let

$$W(t, \mathbf{x}) = \sum_{i,j \geqslant 0} \alpha_{ij} \mathbf{e}_{ij}(\mathbf{x}) \beta_{ij}(t), \tag{2.1}$$

where α_{ij} are coefficients to be determined, β_{ij} are independent standard Brownian motions, and $\mathbf{e}_{ij}(\mathbf{x}) = \mathbf{e}_i(x)\mathbf{e}_j(y)$ where $\mathbf{x} = (x, y)^{\mathrm{T}}$,

$$\mathbf{e}_0(x) = \sqrt{1/L}, \quad \mathbf{e}_j(x) = \sqrt{2/L}\,\cos(\pi j x/L), \quad j = 1, 2, 3, \ldots$$

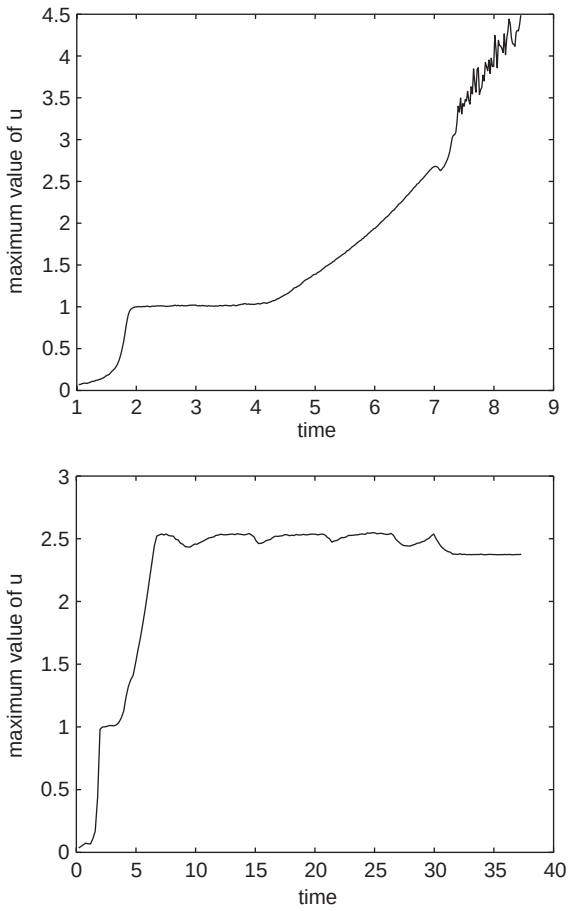

Fig. 5. Plot of $\| u\|_\infty$ against time for numerical solutions of (1.4) with zero initial data. The left hand plot uses an explicit method to simulate the reaction kinetics, the right hand uses implicit. Parameter values: $a=0.75$, $b=0.01$, $D=1$, $L=40$, $\varepsilon=0.02$, $\sigma=0.1$, and correlation length $\xi=2$, with 128^2 grid points and time step 0.01. The $u=1$ plateau indicates wave formation that is coherent for a period of time, but which becomes unstable.

are the orthonormal eigenfunctions of the Laplacian on $[0, L]$ with Neumann boundary conditions. We derive coefficients α_{ij}, so that

$$\mathbf{E}W(t,\mathbf{x})W(t',\mathbf{x}') \approx C(\mathbf{x}-\mathbf{x}')\min\{t,t'\}, \quad C(\mathbf{x}) = \frac{1}{4\xi^2}\exp\left(-\frac{\pi}{4}\frac{\|\mathbf{x}\|^2}{\xi^2}\right),$$

where $\|\cdot\|$ is the standard Euclidean norm, $\mathbf{E}$ denotes expectation, ξ is the spatial correlation length, and $C(\mathbf{x})$ describes the spatial correlation. When $\|\mathbf{x}-\mathbf{x}'\|$ is much bigger than ξ, $C(\mathbf{x}-\mathbf{x}') \approx 0$ and there is no correlation between $W(t,\mathbf{x})$ and $W(t,\mathbf{x}')$. For $\|\mathbf{x}'-\mathbf{x}\| < \xi$, there is correlation, indicating that random fluctuations effect the excitable media over a particular length scale. As $\xi \to 0$, C approaches a δ function and the noise $W(t,\mathbf{x})$ approaches space-time white noise, with no correlation between distinct points. As the correlation length tends to zero, the amount of energy in the Wiener process goes to infinity

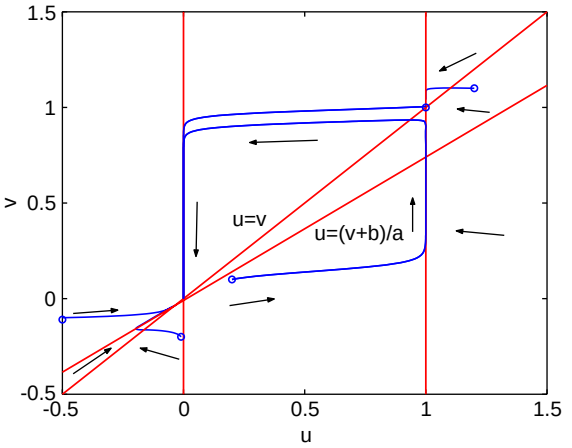

Fig. 6. Illustration of dynamics of $\frac{\mathrm{d}u}{\mathrm{d}t} = \tilde{f}(u, v)/\varepsilon$, $\frac{\mathrm{d}v}{\mathrm{d}t} = \tilde{g}(u, v)$ for $a = 0.75$, $b = 0.01$, $\varepsilon = 0.02$. The arrows illustrate the vector field. For initial condition $(0.2, 0.1)$, the system performs an excursion as before. For initial condition $(1.2, 1.1)$, the solution converge to the fixed point $(1, 1)$.

and this makes it hard or impossible to develop an existence and uniqueness theory for the stochastic PDE with $\xi = 0$; see [7]. To perturb the equations and keep the existing deterministic dynamics in mind, we will choose small but nonzero ξ and σ ($\xi \ll L$ and $\sigma \ll 1$).

We now compute α_{ij} in expansion (2.1). For any Brownian motion $\beta(t)$, $\mathbf{E}\beta(t)\beta(t') = \min\{t, t'\}$. With the independence of β_{ij}, this provides

$$\mathbf{E}W(t, \mathbf{x})W(t', \mathbf{x}') = \min\{t, t'\} \sum_{i,j \geqslant 0} \alpha_{ij}^2 \mathbf{e}_{ij}(\mathbf{x})\mathbf{e}_{ij}(\mathbf{x}').$$

Set $\mathbf{x}' = 0$ and $t = t'$ and multiply by $\mathbf{e}_{k\ell}(\mathbf{x})$ and integrate over $\mathbf{x}$:

$$t \int_0^L \int_0^L C(\mathbf{x})\mathbf{e}_{k\ell}(\mathbf{x})\,\mathrm{d}\mathbf{x} \approx \alpha_{k\ell}^2 \mathbf{e}_{k\ell}(0)t.$$

To enable explicit computation of $\alpha_{k\ell}$, we assume $\xi \ll L$ and take $\mathbf{x}$ away from the boundary. Because of the strong exponential decay, the integrals on $[0, L]$ can be approximated by those on the whole domain, which may be evaluated exactly. Thus, we define

$$\begin{aligned}\alpha_{k\ell}^2 &= \frac{1}{\mathbf{e}_{k\ell}(0)} \int_{\mathbf{R}^2} \frac{1}{4\xi^2} \exp\left(-\frac{\pi}{4} \frac{\|\mathbf{x}\|^2}{\xi^2}\right) \mathbf{e}_{k\ell}(\mathbf{x})\,\mathrm{d}\mathbf{x} \\ &= \frac{1}{4\xi^2} \frac{1}{\mathbf{e}_{k\ell}(0)} \int_{-\infty}^{\infty} \exp\left(-\frac{\pi}{4} \frac{x^2}{\xi^2}\right) \mathbf{e}_k(x)\,\mathrm{d}x \int_{-\infty}^{\infty} \exp\left(-\frac{\pi}{4} \frac{x^2}{\xi^2}\right) \mathbf{e}_\ell(x)\,\mathrm{d}x.\end{aligned}$$

It can be verified that

$$\int_{-\infty}^{\infty} \exp\left(\frac{-\pi x^2}{4\xi^2}\right) \cos(\lambda x)\,\mathrm{d}x = 2\xi \exp\left(\frac{-\lambda^2 \xi^2}{\pi}\right).$$

Let $\lambda_{k\ell} = (\pi/L)^2(k^2 + \ell^2)$, so that $\nabla^2 \mathbf{e}_{k\ell} = -\lambda_{k\ell}\mathbf{e}_{k\ell}$. Then

$$\alpha_{k\ell}^2 = \exp\left(\frac{-\lambda_{k\ell}\xi^2}{\pi}\right). \tag{2.2}$$

The noise $W(t,\mathbf{x})$ defined by (2.1) satisfies

$$\mathbf{E}W(t,\mathbf{x})W(t',\mathbf{x}') = C(\mathbf{x}-\mathbf{x}')\min\{t,t'\} + \text{correction on boundary}.$$

This type of noise is discussed in Garcia-Ojalvo and Sancho [11].

3. Numerical methods

How should the stochastic PDE (1.4) be simulated numerically? The basic finite difference update rule for this type of equation is of the following form: for a time step Δt, we seek approximation u_{ij}^n, v_{ij}^n for $i,j = 0,\ldots,N-1$ at time $n\Delta t$ to $u(x_i,y_j)$, $v(x_i,y_j)$ where (x_i,y_j) is the spatial grid. We use $\mathbf{u}^n$ to denote the matrix u_{ij}^n, $i,j = 0,\ldots,N-1$. The update rule is

$$\begin{aligned} u_{ij}^{n+1} &= u_{ij}^n + D(A\mathbf{u}^n)_{ij}\Delta t + (\Delta t/\varepsilon) f(u_{ij}^n, v_{ij}^n) + \sigma W_{ij}^n, \\ v_{ij}^{n+1} &= v_{ij}^n + \Delta t g(u_{ij}^n, v_{ij}^n), \end{aligned}$$

where A approximates the Laplacian on the grid, and the random variable W_{ij}^n is an approximation to

$$\int_{n\Delta t}^{(n+1)\Delta t} \mathrm{d}W(t,(x_i,x_j)). \tag{3.1}$$

We now discuss the detailed implementation of this method by choosing an approximation to the Laplacian and showing how W_{ij}^n can be approximated efficiently.

3.1. Approximating the Wiener process

First, we wish to exploit the very rapid decay in Fourier coefficients in expansion (2.1). The idea is contained in the following lemma.

Lemma 1. *For an integer $M > 0$, consider the solutions $u(t)$ and $u^M(t)$ of*

$$\begin{aligned} \mathrm{d}u(t) &= \nabla^2 u(t)\,\mathrm{d}t + \mathrm{d}W(t,\mathbf{x}), \quad u(0) = 0, \\ \mathrm{d}u^M(t) &= \nabla^2 u^M(t)\,\mathrm{d}t + \mathrm{d}W^M(t,\mathbf{x}), \quad u^M(0) = 0, \end{aligned}$$

subject to homogeneous Neumann boundary conditions on $[0,L]^2$ where $W^M(t,\mathbf{x})$ is the Wiener process

$$W^M(t,\mathbf{x}) = \sum_{i,j=0}^{M-1} \alpha_{ij}\mathbf{e}_{ij}(\mathbf{x})\beta_{ij}(t). \tag{3.2}$$

Then,

$$\mathbf{E}\,\|\,u(t) - u^M(t)\|_{L_2([0,L]^2)}^2 \leqslant \frac{1}{8\lambda_{M0}}\frac{L^2}{\xi^2}\exp\left(-\pi(M-1)^2\frac{\xi^2}{L^2}\right).$$

Proof. By the Variation of Constants formula

$$u(t) - u^M(t) = \sum_{(i,j)\in\mathscr{M}} \int_0^t \alpha_{ij}\, \mathrm{e}^{-\lambda_{ij}(t-s)} \mathbf{e}_{ij}\, \mathrm{d}\beta_{ij}(s),$$

where the sum is taken over the set $\mathscr{M}$ of positive integers i, j with one of i, $j \geqslant M$. The Itô Isometry yields

$$\mathbf{E} \parallel u(t) - u^M(t) \parallel^2_{L_2([0,L]^2)} = \sum_{(i,j)\in\mathscr{M}} \int_0^t \alpha_{ij}^2\, \mathrm{e}^{-2\lambda_{ij}(t-s)}\, \mathrm{d}s \leqslant \sum_{(i,j)\in\mathscr{M}} \frac{\alpha_{ij}^2}{2\lambda_{ij}}. \tag{3.3}$$

Each λ_{ij} in this sum is bounded from below by $\lambda_{M,0}$. The sum over the α_{ij}^2 is bounded by an integral on the exterior of a circle of radius $M-1$:

$$\sum_{(i,j)\in\mathscr{M}} \alpha_{ij}^2 \leqslant \frac{1}{4} \int_{\|(x,y)\| \geqslant M-1} \mathrm{e}^{-\pi\|(x,y)\|^2\xi^2/L^2}\, \mathrm{d}x\, \mathrm{d}y \leqslant \exp\left(\frac{-\pi(M-1)^2\xi^2}{L^2}\right) \frac{L^2}{4\xi^2}, \tag{3.4}$$

using the definition of α_{ij} in (2.2) and $\int_R^\infty \int_0^{2\pi} \mathrm{e}^{-(x^2+y^2)/a} r\, \mathrm{d}r\, \mathrm{d}\theta = \pi a \mathrm{e}^{-R^2/a}$. Together (3.3) and (3.4) complete the proof. □

This lemma describes how truncating the Fourier expansion of the Wiener process changes the solution of a linear stochastic PDE. Such results can be generalised to semi-linear PDEs, using standard techniques (see for example [21]). We use the error in the approximation to select a suitable truncation of the Wiener process. The discrete L_2 error estimate for a deterministic semi linear heat equation with standard five point approximation to the Laplacian is of the form $\mathscr{O}(\Delta x^2 + \Delta t)$, where Δx denotes the spacing of a uniform grid. When the stochastic forcing is white in time and correlated strongly in space as in (2.1), the root mean square error estimate is typically of the form $\mathscr{O}(\Delta x^2 + \Delta t^{1/2})$ [14] (in some problems with additive noise, it is possible to get $\mathscr{O}(\Delta t)$ rates of convergence; see [18]). Thus, choosing $\Delta t/\Delta x^2$ fixed, the estimate becomes $\mathscr{O}(\Delta x)$ and using the lemma it is appropriate to truncate the expansion by taking the smallest M such that

$$\frac{1}{8D\lambda_{M0}} \frac{L^2}{\xi^2} \exp\left(-\pi(M-1)^2 \frac{\xi^2}{L^2}\right) \leqslant c\Delta x^2 \tag{3.5}$$

some constant c. For N large, this can always be achieved with $M < N$. In fact, this can often be achieved by taking $M \ll N$ even when $\xi \ll L$. Consider for example $L = 80$, $\xi = 2$, $N = 256$, $\Delta x = L/N$ yielding $\Delta x^2 = 9.7656 \times 10^{-2}$ whilst the LHS of (3.5) for $M = 128$ equals 8.9×10^{-11}.

For Eq. (1.4), we have in mind the noise intensity $\sigma \ll 1$. Thus, σ could be used in Eq. (3.5) to achieve some further smallness on the LHS. However, this could lead to choosing zero Fourier modes for the noise which eliminates large deviation behaviour important in the nucleation of waves. Even if the probability of the noise being significant is small we would like to include it and this does not happen if M is too small.

By using the truncated Wiener process defined in (3.2), we can easily generate an approximation to W_{ij}^n by using the FFT. Consider Neumann boundary conditions and choose the spatial grid $x_k = (k + \frac{1}{2})L/N$

and $y_k = (k + \frac{1}{2})L/N$ for $k = 0, \ldots, N-1$. Substituting for $\mathbf{x}$ and truncating to M^2 terms in (2.1), we form approximation (3.1)

$$\sigma W_{k\ell}^n = \sum_{i,j=0}^{M-1} \mathbf{e}_{k\ell,ij} \hat{\alpha}_{ij} w_{ij}^n, \tag{3.6}$$

where w_{ij}^n are independent Gaussian random variables with mean 0 and variance $\sigma^2 \Delta t / L^2$, and $\mathbf{e}_{k\ell,ij} = \mathbf{e}_{k,i}\mathbf{e}_{\ell,j}$, where

$$\mathbf{e}_{k,0} = 1, \quad \mathbf{e}_{k,i} = 2\cos(\pi i(k+1/2)/N), \quad i \neq 0$$

and

$$\hat{\alpha}_{ij} = \exp\left[\frac{-\lambda_{ij}\xi^2}{2\pi}\right] \times \begin{cases} 1, & i = j = 0, \\ 1/\sqrt{2}, & \text{one of } i, j \text{ equals zero}, \\ 1/2, & \text{otherwise}. \end{cases}$$

Given $\hat{\alpha}_{ij}$ and w_{ij}^n, expression (3.6) can be computed using the FFTW3.0 [10] routine DCT-III. In the appendix, we show how the FFT should be used to generate the Wiener process for periodic boundary conditions.

We require M^2 independent samples from a Gaussian distribution at each time step. Even with truncating the $W(t, \mathbf{x})$ expansion from $N = 256$ to $M = 128$ Fourier modes per spatial dimension, a factor of four saving in the number of Gaussian random variables, there are 16,384 samples to be made each time step and it is still important to generate the random variables efficiently. In experiments, we choose the recent Ziggurat method of Marsaglia and Tsang [19], which uses a set of look up tables to significantly improve speed in comparison to the established methods of Box-Mueller and Polar-Marsaglia methods [17] (by a factor of four). Some authors recommend using a three point distribution approximation to the Gaussian and prove convergence in the weak sense in this case. There appears to be no advantage to such a scheme in the present setting.

3.2. Approximating the Laplacian

The PDE (1.1) was introduced as a computationally convenient model of spiral waves. A numerical method was provided to take advantage of the structure of the PDE along with an efficient implementation [3]. The numerical method takes advantage of the shape of the typical u field, which is zero away from a wave, by updating the Laplacian approximation only at grid points where u is bigger than some threshold δ. Thus, we take $A_b\mathbf{u} = A\pi\mathbf{u}$, where $(\pi\mathbf{u})_{ij} = 0$ if $u_{ij} < \delta$ and $=u_{ij}$ otherwise. Barkley uses a nine point approximation A to the Laplacian, which has better stability than a five point approximation. The update rule for $i, j = 0, \ldots, N-1$ is

$$u_{ij}^{n+1} = \begin{cases} u_{ij}^n + D(A_b\mathbf{u}^n)_{ij}\Delta t + (\Delta t/\varepsilon) f(u_{ij}^n, v_{ij}^n), & u_{ij}^n > \delta, \\ D(A_b\mathbf{u}^n)_{ij}\Delta t, & \text{otherwise}, \end{cases}$$

$$v_{ij}^{n+1} = v_{ij}^n + \begin{cases} \Delta t\, g(u_{ij}^n, v_{ij}^n), & u_{ij}^n > \delta, \\ \Delta t\, g(0, v_{ij}^n), & \text{otherwise}. \end{cases} \tag{3.7}$$

We generalise this algorithm to (1.4) in the following manner, which we will refer to as method M1:

$$u_{ij}^{n+1} = u_{ij}^n + \sigma W_{ij}^n + \begin{cases} D(A_{\mathrm{b}}\mathbf{u}^n)_{ij}\Delta t + (\Delta t/\varepsilon) f(u_{ij}^n, v_{ij}^n), & |u_{ij}^n| > \delta, \\ D(A_{\mathrm{b}}\mathbf{u}^n)_{ij}\Delta t, & \text{otherwise}, \end{cases}$$

$$v_{ij}^{n+1} = v_{ij}^n + \begin{cases} \Delta t g(u_{ij}^n, v_{ij}^n), & |u_{ij}^n| > \delta, \\ \Delta t g(0, v_{ij}^n), & \text{otherwise}. \end{cases} \tag{3.8}$$

Notice absolute value signs have been used to determine which update to use and u_{ij}^n is added to u_{ij}^{n+1} in all cases. These changes are cheap to implement and are important as we cannot guarantee that u_{ij}^n will not be large and negative in the presence of noise.

Given our approach to generating W_{ij}^n, it is natural to look for a spectral approximation to ∇^2. By applying a splitting method, we can approximate ∇^2 by calculating one extra FFT and one multiplication by the diagonal matrix of eigenvalues. Specifically, we will consider the following method M2:

(1) Compute coefficients $\hat{u}_{ij}^n$ by the FFT such that $u_{ij}^n = \sum_{k,\ell=0}^{N-1} \hat{u}_{k\ell}^n \mathbf{e}_{k\ell,ij}$. Update

$$\hat{u}_{ij}^{n+1/2} = \begin{cases} \exp(-D\lambda_{ij}\Delta t)(\hat{u}_{ij}^n + \alpha_{ij} w_{ij}^n), & i, j < M, \\ \exp(-D\lambda_{ij}\Delta t)\hat{u}_{ij}^n, & \text{otherwise}. \end{cases}$$

Calculate $u_{ij}^{n+1/2}$ as the inverse transform of $\hat{u}_{ij}^{n+1/2}$.

(2) Apply reaction terms

$$u_{ij}^{n+1} = u_{ij}^{n+1/2} + (\Delta t/\varepsilon) f(u_{ij}^{n+1/2}, v_{ij}^n),$$
$$v_{ij}^{n+1} = v_{ij}^n + \Delta t g(u_{ij}^{n+1/2}, v_{ij}^n).$$

We have chosen to approximate the diffusion and noise terms by the method described in [18], where a higher order convergence rate is proved for a one dimensional example.

Fig. 7 indicates the efficiency of the two methods, along with different choices of M and δ. We see for the case $\sigma = 0$ that method M1 is most efficient. For $N = 512$, M1 is four times faster than M2 and three times faster than $M1$ with $\delta = 0$. Under the cut off, we compute the Laplacian only on a fraction of the spatial domain and this leads to more dramatic results as N is increased. The dependence on the accuracy of M1 on the choice of δ has not been investigated, but it is clear that δ should be made smaller as N is increased.

Consider now $\sigma \neq 0$. The behaviour of the thresholding method M1 becomes progressively worse as the noise level is increased, as the field u is rarely below the threshold δ. We see method M2 is most efficient in this case, though the difference depends on N. Further, the truncated Wiener process (3.2) is shown to give a 10% improvement in performance.

Similar results are obtained with periodic boundary conditions. The noticeable difference in this case is that, under FFTW3.0, it is much faster to use periodic boundary conditions.

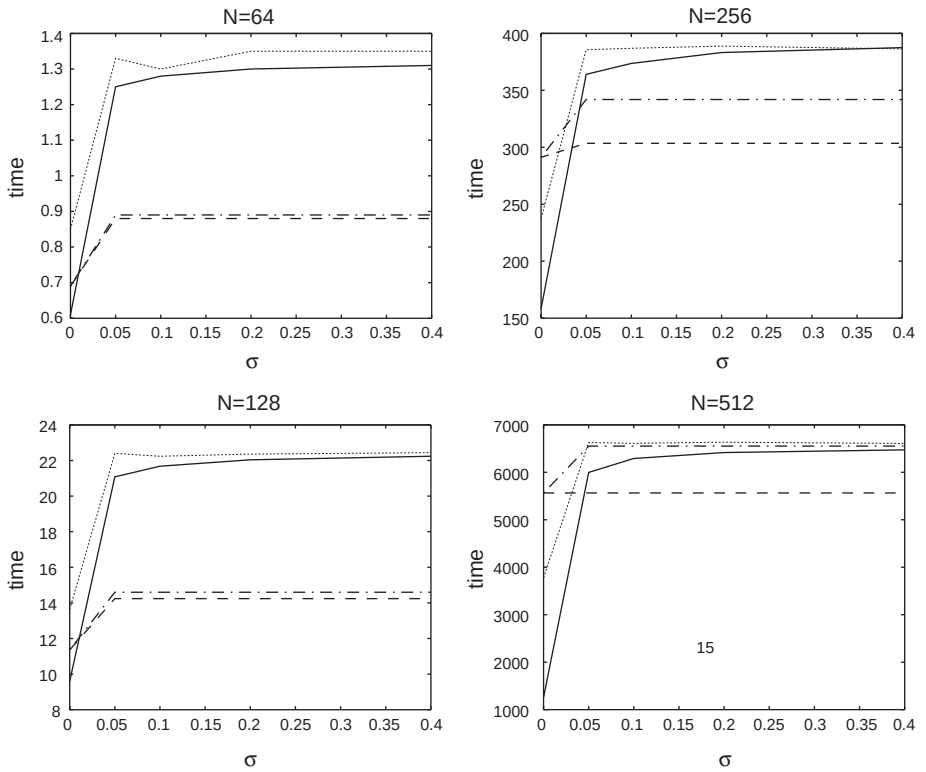

Fig. 7. Time to compute to time $T = 30$ with $\Delta t/\Delta x^2 = 0.02$ against σ for $N = 64, 128, 256, 512$. Plots are given for M1 with $\delta = 0.001$ (solid line), M1 with $\delta = 0$ (dotted line), M2 (dashed line). Each of these methods generates the noise choosing M from (3.5) with $c = 10^{-6}$. To compare timings for M2 without truncation of the Wiener Process are shown (dash dotted line). Parameter values used are $L = 80$, $\varepsilon = 0.02$, $a = 0.75$, $b = 0.01$, $D = 1$.

There are no known exact solutions for this problem and it is therefore difficult to evaluate the error in computing solutions numerically and to compare the relative accuracy of the two methods. The qualitative behaviour of the two methods is observed to be the same in the examples given for $N = 128$.

4. Numerical solution of (1.7)

In examining the numerical solution of (1.4) in detail in the previous subsection, we arrive at recommendations for the numerical simulation of (1.7). It remains effective to use the truncation of the Wiener process in (3.2). But there are different considerations in approximating the Laplacian.

The generalisations to (1.7) of the methods for (1.4) are the following explicit method, which we denote M1′,

$$u_{ij}^{n+1} = u_{ij}^{n} + \begin{cases} D(A_{\mathrm{b}}\mathbf{u}^n)_{ij}\Delta t + (\Delta t/\varepsilon) f(u_{ij}^n, v_{ij}^n), & |u_{ij}^n| > \delta, \\ D(A_{\mathrm{b}}\mathbf{u}^n)_{ij}\Delta t, & \text{otherwise}, \end{cases}$$

$$v_{ij}^{n+1} = v_{ij}^n + \sigma u_{ij}^n W_{ij}^n + \begin{cases} \Delta t g(u_{ij}^n, v_{ij}^n), & |u_{ij}^n| > \delta, \\ \Delta t g(0, v_{ij}^n), & \text{otherwise} \end{cases} \tag{4.1}$$

and the spectral method M2′,

(1) Compute coefficients $\hat{u}_{ij}^n$ by the FFT such that $u_{ij}^n = \sum_{k,\ell=0}^{N-1} \hat{u}_{k\ell}^n e_{k\ell,ij}$. Update

$$\hat{u}_{ij}^{n+1/2} = \exp(-D\lambda_{ij}\Delta t)\hat{u}_{ij}^n.$$

Calculate $u_{ij}^{n+1/2}$ as the inverse transform of $\hat{u}_{ij}^{n+1/2}$.

(2) Apply reaction terms and noise:

$$u_{ij}^{n+1} = u_{ij}^{n+1/2} + (\Delta t/\varepsilon)\, f(u_{ij}^{n+1/2}, v_{ij}^n),$$
$$v_{ij}^{n+1} = v_{ij}^n + \Delta t g(u_{ij}^{n+1/2}, v_{ij}^n) + \sigma u_{ij}^{n+1/2} W_{ij}^n.$$

To apply this spectral method, three FFTs are required to update u_{ij}^n and v_{ij}^n at each time step, two for the Laplacian and one to generate the noise. Thus, for a given time step and spatial resolution, the cost of computing one step of M2′ compared to M2 has increased, whilst the cost of computing with M1′ is unchanged.

Fig. 8 shows timings for a simulation using these methods. We observe that M1′ is much faster as it can take advantage of the smooth regions $u \approx 0$. For (1.7), significant noise only appears when $u \approx 1$ and therefore the regions where $u \approx 0$ are not effected by noise. Strangely, an increasing noise level allows for faster simulation by M1′ in some case. For the resolution $N = 128$, the noise at intensity $\sigma = 8$ causes much of the excitation to die away and much of the spatial domain is near to the equilibrium $u = 0 = v$. Under this situation, the switch in the definition of M1′ is activated and faster simulations are observed. Simulating the same system for resolution $N = 512$, this does not happen on the time scale being examined. It is clear that one must be very careful to resolve all the dynamics in the system, and not consider speed of simulation only.

The choice of reaction term appears less important than in (1.4). For (1.7), it is observed that the reaction terms (1.2) can be simulated for large time scales without instability. It would be interesting to try and prove the equations are well posed over long time.

5. Conclusion

We have reviewed the use of noise in the modelling of excitable media, emphasising the Barkley PDE forced by a space-time Wiener process. For additive noise in the excitation field u, we demonstrated the benefits of modifying the reaction term used in an existing model. Without the modification, the level of excitation u may leave the interval $[0, 1]$ and become much larger than one. This happens for numerical simulations, even with an implicit numerical method.

We considered a spatially correlated noise and suggested an efficient way of generating sampling paths by using the Fourier expansion to reduce the number of Gaussian random variables that must be generated.

The best choice of method depends on the PDE and level of noise under consideration. For (1.1) and $\sigma > 0$, it is better to use a spectral method M2, but for (1.7) it is possible to take advantage of the structure

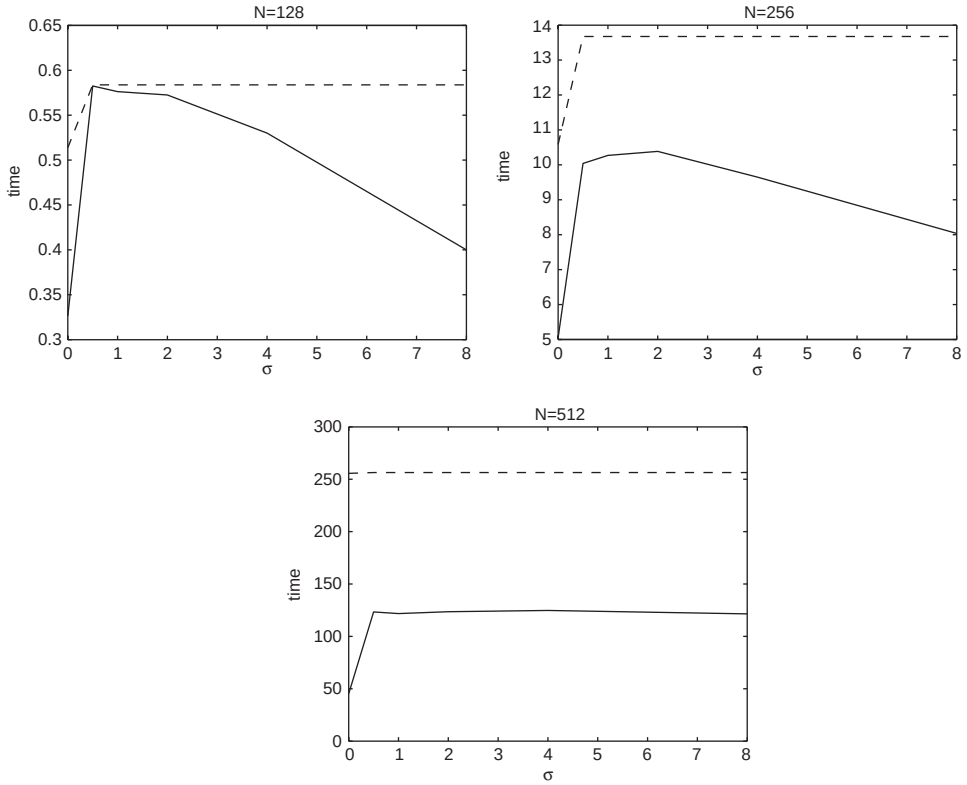

Fig. 8. Time to compute to time $T = 1$ with $\Delta t/\Delta x^2 = 0.02$ against σ for $N = 128, 256, 512$. Plots are given for M1′ with $\delta = 0.001$ (solid line) and M2′ (dashed line). Each of these methods generates the noise choosing M from (3.5) with $c = 10^{-6}$. Parameter values used are $L = 80$, $\varepsilon = 0.02$, $a = 0.75$, $b = 0.01$, $D = 1$.

of the u field using Barkley's approximation to the Laplacian M1′. We noted some spurious behaviour in the solution of (1.7), as excitation in the system decayed away for M1′ at low resolutions and large noise.

Some consideration should be given to an implicit approximation of the reaction term. It should be possible to modify the one suggested in [8] to work with our modified nonlinearity. This was not considered in this paper.

Appendix A. Periodic case

We show how to compute $\sigma W^n_{k\ell}$ with FFT3.0 in the case of periodic boundary conditions. In this case, the expansion of the Wiener process is

$$W(t, \mathbf{x}) = \sum_{i,j \geqslant 0} \sum_{k=1}^{4} \alpha_{ij} \mathbf{e}^k_{ij}(\mathbf{x}) \beta_{ij}(t), \tag{A.1}$$

where α_{ij} are defined by (2.2) with $\lambda_{ij} = (2\pi/L)^2(i^2 + j^2)$. The basis functions $\mathbf{e}^1_{ij}(\mathbf{x}) = \mathbf{e}_i(x)\mathbf{e}_j(y)$, $\mathbf{e}^2_{ij}(\mathbf{x}) = \tilde{\mathbf{e}}_i(x)\mathbf{e}_j(y)$, $\mathbf{e}^3_{ij}(\mathbf{x}) = \mathbf{e}_i(x)\tilde{\mathbf{e}}_j(y)$, and $\mathbf{e}^4_{ij}(\mathbf{x}) = \tilde{\mathbf{e}}_i(x)\tilde{\mathbf{e}}_j(y)$, and $\mathbf{e}_0(x) = \sqrt{1/L}$, $\tilde{\mathbf{e}}_0(x) = 0$,

$$\mathbf{e}_j(x) = \sqrt{2/L}\,\cos(2\pi jx/L), \quad \tilde{\mathbf{e}}_j(x) = \sqrt{2/L}\,\sin(2\pi jx/L), \quad j = 1, 2, 3, \ldots$$

are the orthonormal eigenfunctions of the Laplacian on $[0, L]$ with periodic boundary conditions (we introduce $\tilde{\mathbf{e}}_0 = 0$ for convenience of notation).

Now consider the grid $x_k = kL/N$ and $y_\ell = \ell L/N$ for $k, \ell = 0, \ldots, N-1$. Truncating the series, we define $\sigma W^n_{k\ell}$ by

$$\begin{aligned}
\sigma W^n_{k\ell} = {} & \alpha_{00} w^n_{00,1} + \sqrt{2}\sum_{i=1}^{N/2} \alpha_{i0}(\cos(ki2\pi/N) w^n_{i0,1} + \sin(ki2\pi/N) w^n_{i0,2}) \\
& + \sqrt{2}\sum_{j=1}^{N/2} \alpha_{0j}(\cos(\ell j2\pi/N) w^n_{0j,1} + \sin(\ell j2\pi/N) w^n_{0j,2}) \\
& + 2\sum_{i,j=1}^{N/2} \alpha_{ij}(\cos(ki2\pi/N)\cos(\ell j2\pi/N) w^n_{ij,1} + \cos(ki2\pi/N)\sin(\ell j2\pi/N) w^n_{ij,2} \\
& + \sin(ki2\pi/N)\cos(\ell j2\pi/N) w^n_{ij,3} + \sin(ki2\pi/N)\sin(\ell j2\pi/N) w^n_{ij,4}),
\end{aligned}$$

where $w^n_{ij,k}$ are independent Gaussian random variables with mean 0 and variance $\sigma^2\Delta t/L^2$. This can be re-expressed in terms of complex exponentials, as follows. For $j > 0$,

$$\cos(\ell j2\pi/N) w^n_{ij,2k-1} + \sin(\ell j2\pi/N) w^n_{ij,2k} = \tfrac{1}{2}[z^n_{ij,k} e^{\sqrt{-1}\ell j2\pi/N} + \bar{z}^n_{ij,k} e^{-\sqrt{-1}\ell j2\pi/N}],$$

where $z^n_{ij,k} = w^n_{ij,2k-1} - \sqrt{-1} w^n_{ij,2k}$. Denote the fourth term in σW^n_{kl} by Σ_4, then

$$\begin{aligned}
\Sigma_4 = {} & \sum_{i,j=1}^{N/2} \alpha_{ij}(\cos(ki2\pi/N)[z^n_{ij,1} e^{\sqrt{-1}\ell j2\pi/N} + \bar{z}^n_{ij,1} e^{-\sqrt{-1}\ell j2\pi/N}] \\
& + \sin(ki2\pi/N)[z^n_{ij,2} e^{\sqrt{-1}\ell j2\pi/N} + \bar{z}^n_{ij,2} e^{-\sqrt{-1}\ell j2\pi/N}]).
\end{aligned}$$

Substituting $\cos X = (e^{\sqrt{-1}X} + e^{-\sqrt{-1}X})/2$ and $\sin X = -\sqrt{-1}(e^{\sqrt{-1}X} - e^{-\sqrt{-1}X})/2$

$$\begin{aligned}
\Sigma_4 = {} & \frac{1}{2}\sum_{i,j=1}^{N/2} \alpha_{ij}(e^{\sqrt{-1}ki2\pi/N} e^{\sqrt{-1}\ell j2\pi/N}[z^n_{ij,1} - \sqrt{-1} z^n_{ij,2}] \\
& + e^{\sqrt{-1}ki2\pi/N} e^{-\sqrt{-1}\ell j2\pi/N}[\bar{z}^n_{ij,1} - \sqrt{-1}\bar{z}^n_{ij,2}] \\
& + e^{-\sqrt{-1}ki2\pi/N} e^{\sqrt{-1}\ell j2\pi/N}[z^n_{ij,1} + \sqrt{-1} z^n_{ij,2}] \\
& + e^{-\sqrt{-1}ki2\pi/N} e^{-\sqrt{-1}\ell j2\pi/N}[\bar{z}^n_{ij,1} + \sqrt{-1}\bar{z}^n_{ij,2}]).
\end{aligned}$$

Similarly, the third term can be written

$$\Sigma_3 = \frac{1}{\sqrt{2}} \sum_{j=1}^{N/2} \alpha_{0j} (\mathrm{e}^{\sqrt{-1}\ell j 2\pi/N} z^n_{0j,1} + \mathrm{e}^{-\sqrt{-1}\ell j 2\pi/N} \bar{z}^n_{0j,1})$$

and the second term

$$\Sigma_2 = \frac{1}{\sqrt{2}} \sum_{i=1}^{N/2} \alpha_{i0} (\mathrm{e}^{\sqrt{-1}ki 2\pi/N} z^n_{i0,1} + \mathrm{e}^{-\sqrt{-1}ki 2\pi/N} \bar{z}^n_{i0,1}).$$

The whole sum now be rewritten in the standard form, convenient for the FFTW3.0 DFT transform,

$$\sigma W^n_{k\ell} = \sum_{i,j=0}^{N-1} \hat{\alpha}_{ij} Z^n_{ij} \mathrm{e}^{\sqrt{-1}ki 2\pi/N} \mathrm{e}^{\sqrt{-1}\ell j 2\pi/N},$$

where for $i, j = 1, \ldots, N/2$

$$\hat{\alpha}_{00} = 1, \quad \hat{\alpha}_{i0} = \alpha_{i0}/\sqrt{2}, \quad \hat{\alpha}_{0j} = \alpha_{0j}/\sqrt{2}, \quad \hat{\alpha}_{ij} = \hat{\alpha}_{N-i,j} = \alpha_{ij}/2$$

and

$$Z^n_{00} = w^n_{00}, \quad Z^n_{0j} = z^n_{0j,1}, \quad Z^n_{0,N-j} = \bar{z}^n_{0j,1}, \quad Z^n_{i0} = z^n_{i0,1}, \quad Z^n_{N-i,0} = \bar{z}^n_{i0,1}$$

and

$$Z^n_{ij} = z^n_{ij,1} - \sqrt{-1} z^n_{ij,2}, \quad Z^n_{N-i,j} = z^n_{ij,1} - \sqrt{-1} z^n_{ij,2}.$$

The remaining coefficients are defined by the symmetry $\hat{\alpha}_{ij} = \hat{\alpha}_{N-i,N-j}$ and $Z^n_{ij} = \bar{Z}^n_{N-i,N-j}$. It is simpler to generate Z^n_{ij} for $i, j = 1, \ldots, N/2$ as complex numbers with real and imaginary parts independent $N(0, \sigma^2 \Delta t / L^2)$ random variables, taking modified coefficients $\hat{\alpha}_{ij} = \hat{\alpha}_{N-i,j} = \alpha_{ij}/\sqrt{2}$.

The thresholding algorithm may be applied to periodic boundary conditions, by summing over (i, j), $(N - i, j)$, $(i, N - j)$, and $(N - i, N - j)$, for $i, j = 0, \ldots, M$. M should be chosen from $0, \ldots, N/2$ such that (3.5) holds, where $\lambda_{M0} = (2\pi/L)^2 M^2$, an eigenvalue of the Laplacian with periodic boundary conditions.

References

[1] S. Alonso, F. Sagues, J.M. Sancho, Excitability transitions and wave dynamics under spatiotemporal structured noise, Phys. Rev. E 65 (066107) (2002) 11.

[2] D. Barkley, A model for fast computer simulation of waves in excitable media, Physica D 49 (1991) 61–70.

[3] D. Barkley, EZ-Spiral, http://www.maths.warwick.ac.uk/barkley/, 2002.

[4] G. Bub, Optical mapping of pacemaker interactions, Ph.D. Thesis, McGill, 2000.

[5] G. Bub, A. Shrier, Propagation through heterogeneous substrates in simple excitable media, Chaos 12 (3) (2002) 747–753.

[6] H. Busch, F. Kaiser, Influence of spatiotemporally correlated nose on structure formation in excitable media, Phys. Rev. E 67 (041105) (2003) 7.

[7] G. Da Prato, J. Zabczyk, Stochastic Equations in Infinite Dimensions, Vol. 44, Encyclopedia of Mathematics and its Applications, Cambridge University Press, Cambridge, 1992.

[8] M. Dowle, R.M. Mantel, D. Barkley, Fast simulations of waves in three-dimensional excitable media, Internat. J. Bifur. Chaos Appl. Sci. Eng. 7 (11) (1997) 2529–2545.
[9] R. FitzHugh, Mathematical models of threshold phenomena in the nerve membrane, Math. Biophys. 17 (1955) 257–278.
[10] M. Frigo, S.G. Johnson, FFTW: an adaptive software architecture for the FFT, Proc. ICASSP 3 (1998) 1381–1384.
[11] J. García-Ojalvo, J.M. Sancho, Noise in Spatially Extended Systems, Springer, Berlin, 1999.
[12] J. Garcia-Ojalvo, L. Schimansky-Geier, Noise-induced spiral dynamics in excitable media, Europhys. Lett. 47 (3) (1999) 298–303.
[13] J.M. Greenberg, S.P. Hastings, Spatial patterns for discrete models of diffusion in excitable media, SIAM J. Appl. Math. 34 (3) (1978) 515–523.
[14] E. Hausenblas, Approximation for semilinear stochastic evolution equations, Potential Anal. 18 (2) (2003) 141–186.
[15] P. Jung, G. Mayer-Kress, Noise controlled spiral growth in excitable media, Chaos 5 (2) (1994) 458–462.
[16] J.P. Keener, Arrhythmias by dimension, Proc. Sympos. Appl. Math., Amer. Math. Soc., Providence, RI 59 (2002) 57–81.
[17] P.E. Kloeden, E. Platen, Numerical Solution of Stochastic Differential Equations, Applications of Mathematics, Vol. 23, Springer, Berlin, 1992.
[18] G.J. Lord, J. Rougemont, A numerical scheme for stochastic PDEs with Gevrey regularity, IMA J. Num. Anal. 2003, to appear.
[19] G. Marsaglia, W.W. Tsang, The Ziggurat method for generating random variables, Journal of Statistical Software (8) (2000) 7.
[20] G. Moe, W. Rheinboldt, A. Abildskov, A computer model of atrial fibrillation, Am. Heart J. 67 (1964) 200–220.
[21] T. Shardlow, Numerical methods for stochastic parabolic PDEs, Numer. Funct. Anal. Optim. 20 (1–2) (1999) 121–145.
[22] T. Shardlow, Nucleation of waves in an excitable media by noise, SIAM Multiscale Model. Simul., to appear.
[23] K.L. Tomchik, P.N. Deverotes, Adenosine 3′, 5′-monophosphate waves in Dictyolestium discoideum: a demonstration by isotope dilution-fluorography, Science 212 (1981) 443–446.
[24] N. Wiener, A. Rosenblueth, The mathematical formulation of the problem of conduction of impulses in a network of connected excitable elements, Archos. Inst. Cardiol. Mex. 16 (1946) 205–265.
[25] A.T. Winfree, Varieties of spiral wave behavior: an experimentalist's approach to the theory of excitable media, Chaos 1 (1991) 33.
[26] A.N. Zaikin, A.M. Zhabotinsky, Concentration wave propagation in two-dimensional liquid-phase self-oscillating system, Nature 225 (1970) 535.